Micromachined Wideband Ridge Gap Waveguide Power Divider at 220-325 GHz

Citation for the original published paper (version of record):
Farjana, S., Uz Zaman, A., Lundgran, P. et al (2022). Micromachined Wideband Ridge Gap Waveguide Power Divider at 220-325 GHz. IEEE Access, 10: 27432-27439.
http://dx.doi.org/10.1109/ACCESS.2022.3156095

(article starts on next page)

IEEE Access
Multidisciplinary | Rapid Review | Open Access Journal

Received January 19, 2022, accepted February 15, 2022, date of publication March 2, 2022, date of current version March 16, 2022.

Digital Object Identifier 10.1109/ACCESS.2022.3156095

Micromachined Wideband Ridge Gap Waveguide Power Divider at 220-325 GHz

SADIA FARJANA[1], ASHRAF UZ ZAMAN[2], (Senior Member, IEEE), PER LUNDGREN[1], AND PETER ENOKSSON[1,3], (Member, IEEE)

[1]Department of Microtechnology and Nanoscience, Chalmers University of Technology, 41296 Göteborg, Sweden
[2]Department of Electrical Engineering, Chalmers University of Technology, 41296 Göteborg, Sweden
[3]Enoaviatech AB, 11226 Stockholm, Sweden

Corresponding author: Sadia Farjana (farjana@chalmers.se)

This work was supported in part by the Adlerbertska Forskningsstiftelsen Fund, and in part by Swedish Strategic Vehicle Research and Innovation (FFI) Project under Grant 2018-02707.

ABSTRACT A micromachined ridge gap waveguide power divider operating at 220-325 GHz is presented. The device is fabricated by SUEX dry film photoresist. Dry film photoresist can be used to obtain geometrical features with high accuracy using a robust fabrication process. The designed power divider has simple geometrical features and a wide band performance. The measured transmission coefficients are equal to -3.5 ± 0.4 dB at 220-325 GHz and the measured input reflection coefficient is below -12 dB at 220-325 GHz. The measurement results are in good agreement with simulations, demonstrating that the proposed fabrication method is suitable for the fabrication of waveguide components operating at the millimeter and sub-millimeter wave range. The presented low-loss ridge gap waveguide power divider may enable cost-effective and rapid fabrication of passive devices such as high gain antennas operating up to THz frequencies.

INDEX TERMS Dry film photoresist, gap waveguide, micromachining, millimeter wave, power divider, sub-millimeter wave.

I. INTRODUCTION

Recently millimeter-wave (mmWave), and submillimeter-wave (sub-mmWave) technologies have gained increasing attention to provide more available bandwidth and higher capacity [1]. One of the advantages offered by higher frequencies is the reduced size of the waveguide components, which leads to more compact systems. At the same time there are increasing challenges in fabrication of components as the feature size becomes very small. Until now the most used waveguide components manufacturing method is machine-based computer numerical control (CNC) milling. The achievable accuracy by this method is inadequate in many cases, especially for submillimeter-wave frequencies [2]. Additionally, due to the serial nature of the process, the cost for devices built in this way is very high and not suitable for many applications. At this point micromachining offers significantly better precision and flexibility compared to CNC milling. Moreover, micromachining is a parallel process, and offers the potential for low-cost volume production.

The associate editor coordinating the review of this manuscript and approving it for publication was Su Yan.

Different micromachining methods employing silicon-based deep reactive ion etching (DRIE) [3], [4], SU8 photoresist [5], [6], or LIGA (Lithography, Electroplating, and Molding)-based thick layer electroplating [7], [8] have been investigated and utilized for manufacturing of mmWave and sub-mmWave waveguide components. However, these methods suffer from several fabrication issues. A common challenge related to micromachining is the need for several consecutive processing steps, which results in extended production times. Additionally, DRIE suffers from non-vertical and uneven sidewalls [9], [10], the LIGA process suffers from non-uniformities [11] and in the SU-8 process there are challenges with non-planar resist distribution, edge bead and delamination [12], [13]. Dry film photoresist on the other hand can overcome all above-mentioned fabrication issues. Recently SUEX dry film photoresist has been used to fabricate waveguide components operating above 200 GHz [14], verifying that dry film photoresist not only delivers superior geometrical features and fabrication tolerances, but also reduces the processing time and the production cost.

In view of the very demanding requirements on fabrication accuracy at mmWave frequencies, gap waveguide (GW)

technology has proven itself very useful as it lends itself to low complexity manufacturing [15]. The GW offers some benefits over conventional rectangular waveguides (RW) and planar transmission lines such as microstrip lines or substrate integrated waveguides (SIW). A GW structure does not rely on an electrical connection between different parts as the operating principle is based on controlling the boundary condition of a parallel plate mode. By placing a Perfect Electric Conductor (PEC) and a Perfect Magnetic Conductor (PMC) in parallel and by separating the layers by an air gap $<\lambda/4$, the GW technology prohibits wave propagation in an unwanted direction. Also, the wave propagates in air, so GW structures do not suffer from the incorporation of lossy dielectrics.

Different GW components have been designed and demonstrated both at low and high frequency [16]–[18]. Many micromachining techniques such as silicon micromachining technology, SU8 based polymers and injection molding technique have already been used to realize various gap waveguide components such as antennas and transmission lines [19]–[21]. Power dividers are also important components of microwave and millimeter wave circuit design. They work as the fundamental building block for multiplexers, power combiners, and antenna feed networks. Depending on its application a power divider can be used for both dividing and combining power. Some important parameters that define the performance of a power divider is its return loss bandwidth, insertion loss, and amplitude and phase imbalance [22]. Therefore, it is very important that the measurement results can show good agreement with the simulation results. Usually, the defects introduced by the fabrication method has significant effect on the return loss bandwidth and the insertion loss of any fabricated device. Hence the fabrication technique used to fabricate the power divider needs to have high fabrication accuracy for a good match between measurements and simulations.

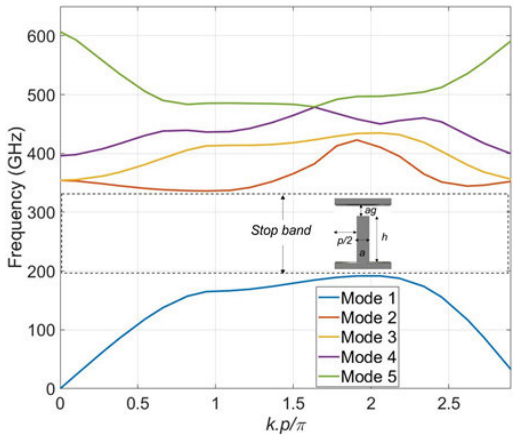

FIGURE 1. Simulated dispersion diagram of an infinite periodic pin cell.

In this paper we demonstrate a ridge gap waveguide (RGW) based power divider fabricated by SUEX dry film photoresist. A benefit of the proposed power divider is that all the structures are of the same height, alleviating the designed power divider from alignment issues introduced by extra fabrication steps, which is very critical at sub-mmWave frequencies. Also, the waveguide ports are connected from the top plate thus making the feeding and excitation less assembly sensitive. The novelty of this work lies in the fact that the proposed micromachining-based fabrication method is less time consuming and more straight-forward than alternative processes.

II. DESIGN OF THE PROPOSED POWER DIVIDER

For the proposed power divider, the waveguide port is located on the top plate. This top plate acts as the PEC surface of the GW structures and the rows of pins of the bottom plate acts as a PMC surface.

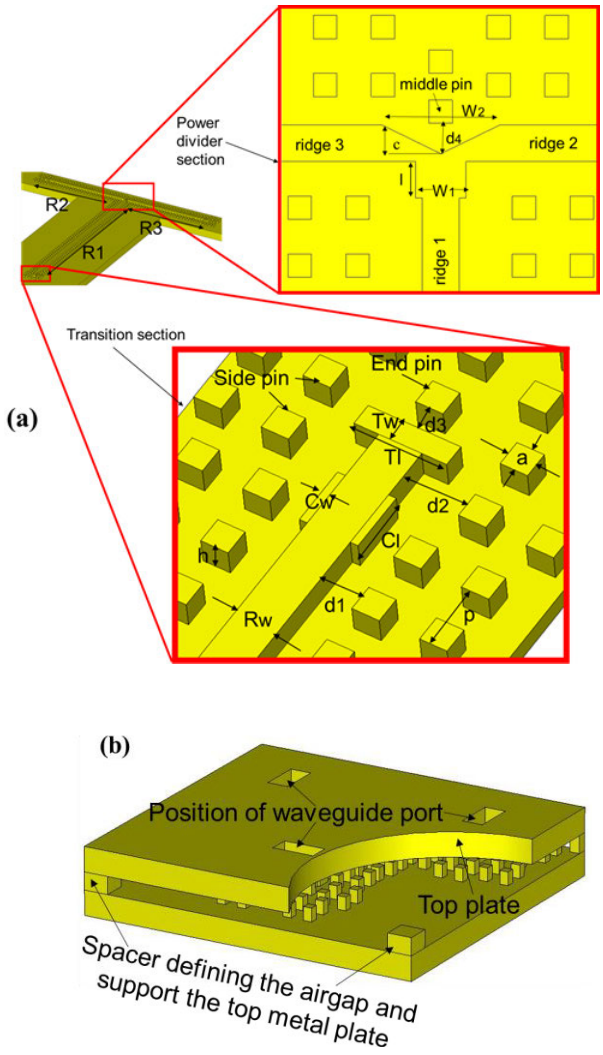

FIGURE 2. Configuration of proposed RGW power divider. (a) Layout of the bottom plate, (b) perspective view of the power divider showing position of waveguide ports, spacers, and top plate.

A transition has been designed to couple the electromagnetic (EM) wave that passes through the standard WR-3.4 RW to propagate through the GW structures. Full-wave electromagnetic simulation of the design is performed

with CST microwave studio. For the designed power divider, the sustained pin height (h) is 270 μm, the pin size (a) is 177 μm, the distance between two pins (p) is 260 μm, and the ridge height (Rh) for the RGW is 270 μm, to achieve a stopband from 200 to 340 GHz. The dispersion diagram of the infinite 2-D pin array are shown in Figure 1. A T-section ridge with a width (T_w) of 150 μm and length (T_l) of 620 μm is added to the main ridge for impedance matching. The width of the main ridge (R_w) is 279 μm. A capacitive stub of width (C_w) 50 μm and length (C_l) 400 μm is also added beside this T-ridge section. The distance (d_2) between the T-section ridge to the T-section side pins has been optimized to 410 μm. To prevent any possible leakage two pins are placed after the T-section. The distance (d_3) between the T-section ridge to the T-section end pin has been optimized to 150 μm for better impedance matching. Figure 2. shows the configuration of the proposed RGW power divider with the described transition. An airgap (ag) of 120 μm is maintained between the pin and the ridge to the top plate. To evaluate the tolerance error, this air gap has been swept 20 μm around this nominal value. The results are shown in Figure 3.

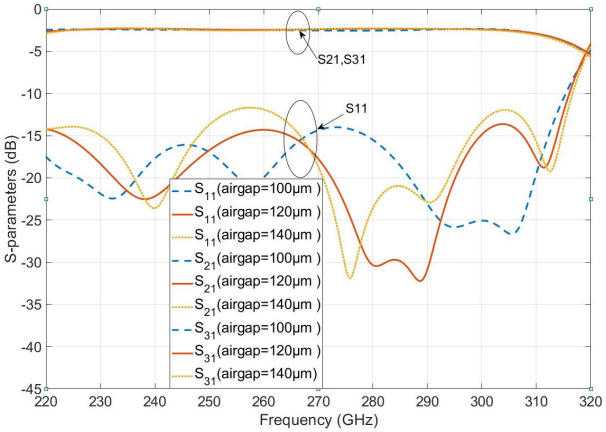

FIGURE 3. Evaluation of the effect on the power divider performance of errors in the airgap.

The designed power divider has a RGW T-junction with two other ridges and pins to match the input port and to split the incoming power from input port to the output ones. The length of ridge 1 (R_1) is 25.5 mm, ridge 2 (R_2) is 13.5 mm long and ridge 3 (R_3) has a length of 13.5 mm. The width of the ridge is varied near the T-junction by dimension l = 275 μm and w_1 = 379 μm to form the $\lambda/4$ section needed for such power divider. Two middle ridges are cut to divide the power equally between these two ridges. The optimized value for the middle section is w_2 = 900 μm and c = 219 μm. The optimization was done considering better input matching, better power distribution between the two ridges and fabrication limitations. The ratio of w_2 : c has been chosen in such a way that during fabrication we do not end up with a rounded corner instead of a sharp corner. Figure 4a and 4b show the optimized value of c and w_2 provide better S_{11} as well as are free of any fabrication constrains. The distance

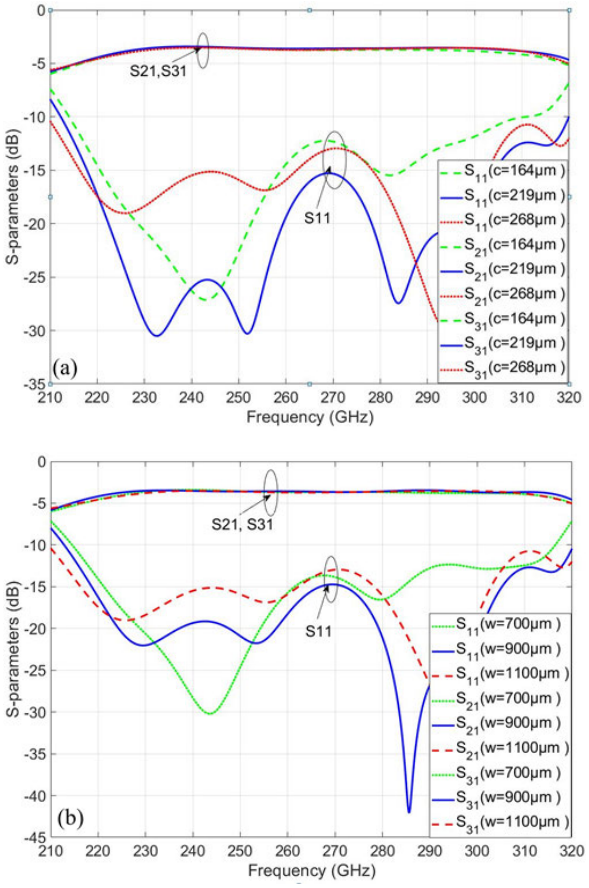

FIGURE 4. Simulated s-parameters of the micromachined RGW power divider against frequency using different optimization value for the T-junction. (a) different values of c, (b) different values of w2.

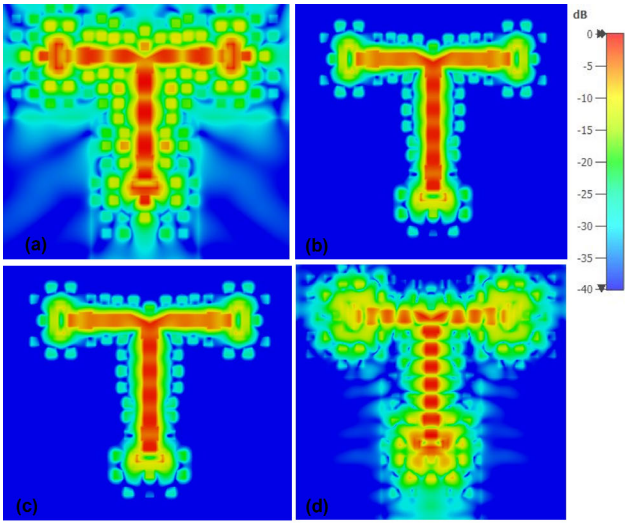

FIGURE 5. Simulated E-field distribution in the power divider at (a) 200 GHz, (b) 230 GHz, (c) 270 GHz, and (d) 350 GHz.

between the middle ridge and the middle pin has been used as a tuning parameter and the distance (d_4) is 230 μm.

During the optimization of all the sensitive parameters, $\pm$10 μm pin height tolerance has been considered also. From our previous experiments on SUEX dry film photoresist

the achieved fabrication tolerance was ± 2 μm [14]. Thus, the designed T-junction power divider is expected to perform well after manufacturing. Figure 5 shows the simulated amplitude of the E-field distribution inside the power divider in four different frequencies (200, 230, 270 and 350 GHz) and it shows there is no significant field leakage in the band of interest from 220-320 GHz.

III. FABRICATION PROCESS

The designed power divider has been fabricated by using SUEX dry film photoresist (DJ MICROLAMINATES Inc.). SUEX dry film photoresist is delivered sandwiched between two polyester (PET) films. A commercial laminator (PRO SERIESTM 3600) has been used to laminate the dry film sheet. The fabrication has been completed in two steps; a base layer formation and the structures have subsequently been fabricated on top of the base layer. Figure 6 shows the schematic of the fabrication process.

A silicon (Si) wafer has been used as a carrier during the lamination process. Before starting the lamination, a plasma cleaning was done followed by a dehydration bake at 200 °C for 15 minutes. A 40 μm SUEX sheet has been laminated on the Si wafer. The laminator temperature has been set to 65 °C and the speed of the lamination has been maintained at 5 mm/sec. The laminated SUEX film has been soft baked at 80 °C for 1 min on a hot plate followed by a flood exposure with an energy of 1200 mJ/cm^2 and a post-exposure bake at 95 °C for 10 min. This fully crosslinked layer was later used as a base layer.

To obtain the structure layer, SUEX dry film sheets of 200 μm, 50 μm, and 20 μm have been used. Those three sheets have been laminated sequentially. After lamination of the 200 μm thick dry film sheet, a post lamination bake at 80 °C for 1 min 30 sec has been conducted on a hot plate to ensure adhesion of the laminated layer with the base dry film layer. Later a 50 μm film and a 20 μm film were laminated and both the lamination processes have been followed by a post lamination bake at 80 °C for 1 min. The 270 μm thick film has been exposed under UV with a mask to obtain the patterns of the device with an exposure energy of 9000 mJ/cm^2. A two-step post-exposure bake was done starting at 65 °C on a hot plate for 10 min and followed by a bake at 95 °C for 1 hr.

The whole wafer has been developed in mr-DEV 600. The development was done in two different baths. The wafer was kept in the first developer bath for 20 mins without any agitation and moved to the second developer bath and kept in the second bath for 20 mins with mild agitation. The development process was then followed by a rinse with an IPA solution where the samples were maintained in the IPA bath for 5 min.

The drying process has been carried out on a hot plate at 100 °C and a hard bake was done at 150 °C for 10 min. The wafer was then diced into pieces. To make the chip conductive, both sides of the structure has been sputtered with 50 nm Ti and 900 nm Au.

One of the attractive features of this dry film process is that it does not require waiting time between each step. Also, the lamination process is quite fast, which makes the overall fabrication time very short compared to other thick liquid photoresist-based microfabrication process.

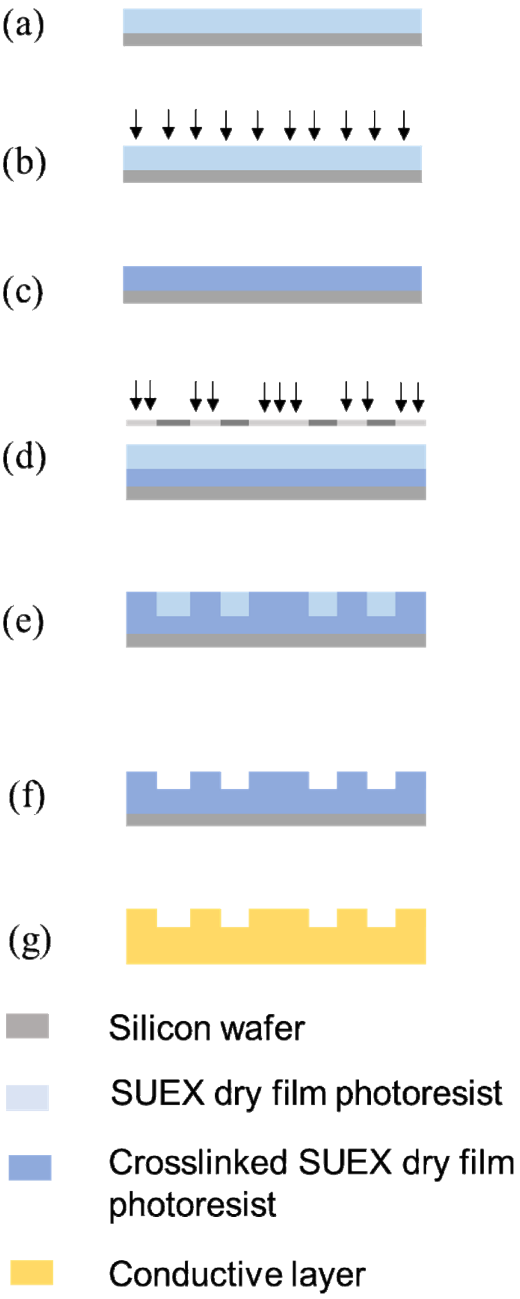

FIGURE 6. Schematic of the complete fabrication process. (a) laminated SUEX dry film sheet on the wafer, (b) flood exposure of the laminated dry film, (c) post exposure baked dry film sheet used as a base layer, (d) lamination of another SUEX sheet on top of the base layer, soft baked and UV exposed with a mask, (e) post-exposure bake of dry film photoresist, (f) patterned dry film after development, (g) sputtering of the final structure.

IV. MEASUREMENT RESULTS AND DISCUSSION

The characterization of the dry film micromachined RGW power divider has been performed using a Keysight

PNA-X network analyzer N5242A and VDI WR 3.4 frequency extender modules. Power dividers are three-port devices. However, due to the availability of a limited number of Tx/Rx ports, for S-parameter characterization, two port measurements were performed separately for the input port and each of the output ports. The remaining output port was terminated with a waveguide load during each measurement. A Through-Reflect-Line (TRL) calibration was carried out using a standard calibration kit. Figure 7 shows the measurement setup for the power divider where two ports are connected to the WR 3.4 frequency extender modules, and the third port is terminated with a load.

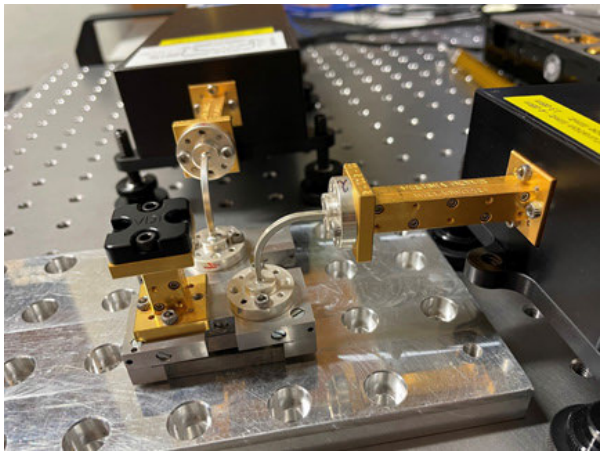

FIGURE 7. Measurement setup.

A. MILLED SUPPORT PACKAGE

Two support packages have been designed and manufactured by CNC milling to support the chip during the measurements. The top part of the support package acts as the metal lid (PEC) above the active area of the micromachined power divider and has the openings for connection to standard WR-3.4 rectangular waveguides. The bottom layer of the support package has a channel for the chip and four spacers at the edge to maintain the required airgap. The sensitivity of the transition performance for misalignment between the ridge and the waveguide port has been evaluated in the previous work presented by the authors and the design was shown to be robust [23]. Figure 8 shows an image of the milled support package.

B. FABRICATION RESULTS

Figure 9 shows the SEM image of the fabricated power divider chip. The fabricated chip contains a base layer and structures on the base layer. The optimized height of the structures was 270 μm. The height of the fabricated structures is 272 $\pm$ 2 μm which is very close to the optimized pin height. This fabrication tolerance is very suitable for the designed transition. The surface roughness of the fabricated chip has a significant effect on the performance of the device. The measured surface roughness of the fabricated chip was 3.25 $\pm$ 0.5 nm, which is suitable at this frequency range.

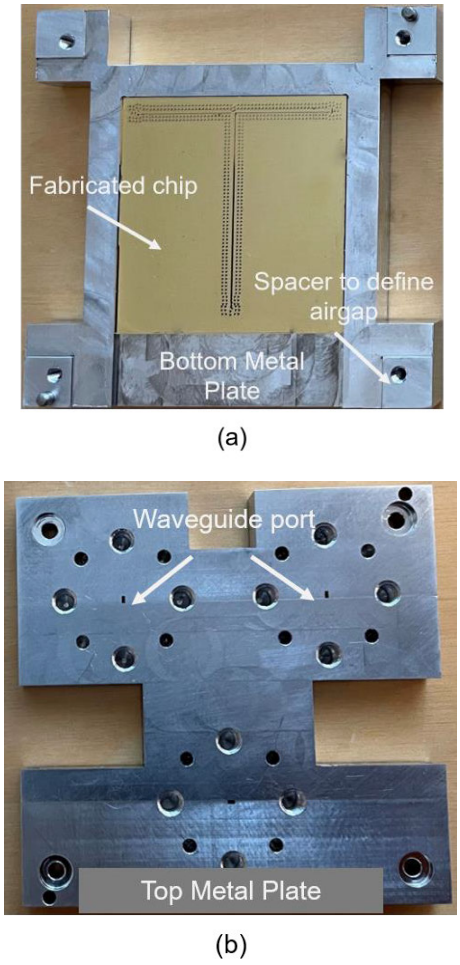

FIGURE 8. Image of the supporting device. (a) bottom plate with the chip. (b) top plate showing the opening for the waveguide port.

C. MEASURMENT RESULTS

The measured and simulated input reflection coefficient, S_{11} and transmission coefficients S_{21} and S_{31} for the dry film photoresist micromachined ridge gap waveguide power divider is presented in Figure 10 and Figure 11. respectively. The measured reflection coefficient is below -12 dB over the frequency band 220–325 GHz, compared to the simulated value of -15 dB. The measured S_{21} and S_{31} from port to port is found to be varying between -5.75 and -6.25 dB and is about 1 dB more than the simulated value over the same band.

The experimental results are found to be in relatively close agreement with the simulated data and the discrepancies are at least in part due to the ideal waveguide sidewall and perfectly smooth ridge surface used in the simulation model. Also, the port-to-port measurement results mentioned above include the losses of the extra ridge gap waveguide line with a length of 24+12 = 36mm which has been added to separate the ports to fit two WR3.4 flanges on the top plate (without overlapping each other) and to make the two

TABLE 1. Comparison Of different state-of-the-art power dividers.

References	Method	Fabrication issues	FBW [%]	f_c [GHZ]	IL* [dB]	RL* [dB]	Imbalance	
							Amp. [dB]	Phase [°]
[24]	CNC	Serial, time intense and costly process	30	100	0.3	NA	0.3	~ 0
[25]	CNC	Serial, time intense and costly process	38	185	0.3	~-20	0.15	~ 0
[4]	DRIE	Time intense process	27	90	< 1.2	< -10	NA	NA
[26]	DRIE	Time intense process	37	270	< 0.9	< -10	NA	~ 0
This Work	Dry film	Fast and simple process	37	270	< 1.0	< -10	0.2	0.8

FBW: Fractional bandwidth, NA: Not available, *IL: Insertion loss, fc: Center frequency, *RL: Return loss, Amp.: Amplitude

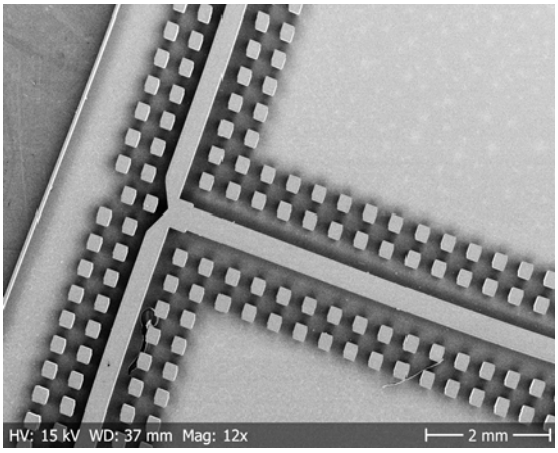

FIGURE 9. SEM image of the fabricated chip with 272 ± 2 μm high structures.

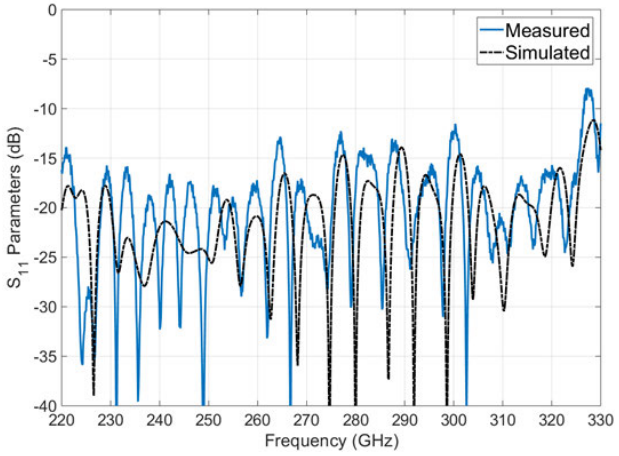

FIGURE 10. Simulated and measured S11 of the RGW power divider.

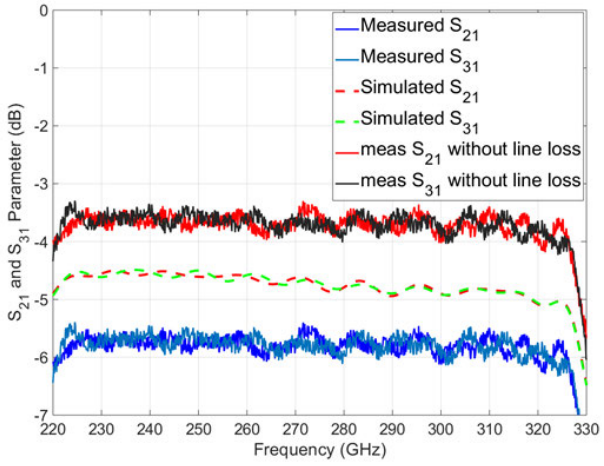

FIGURE 11. Simulated, measured and de-embedded S21 and S31 of micromachined RGW power divider.

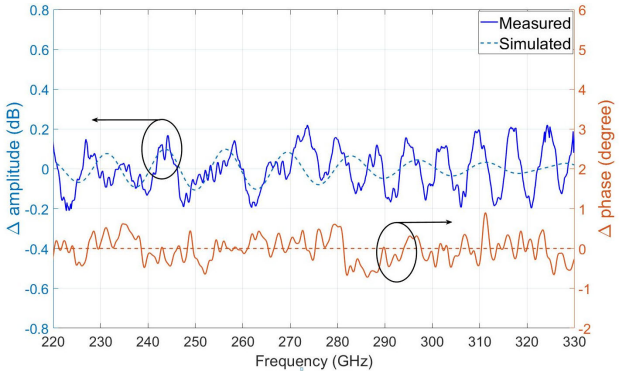

FIGURE 12. Simulated, measured amplitude imbalance and phase imbalance of the power divider.

port measurements. One 25 mm straight ridge gap waveguide section has also been fabricated using the same micromachining process and has been characterized to evaluate the losses in the stand-alone ridge gap waveguide section. Two waveguide E-plane 90° bends have been used in the measurements, and the effect of these bends also have been calibrated out, while calculating the line loss. The line losses in this longer ridge gap waveguide have been found to be

maximum of 0.075 dB/mm over the band of interest from 220-325 GHz [23]. Based on this experimental data, the losses in the extra ridge gap waveguide section of this 3 dB power divider device have been found to be calculated as 2.7 dB for the 36 mm of long ridge section. After de-embedding this extra loss, the maximum insertion losses in the ridge gap waveguide 3 dB power divider section have been found to be within the range of −3.6 to −4.0 dB from 220-325 GHz. This implies a total loss of about 0.5-1 dB from an ideal 3 dB power divider section. This loss value is compared with the losses of other state of the art 3 dB power dividers. Figure 12 shows the simulated and measured amplitude imbalance and phase imbalance. The measured amplitude and phase imbalance are better than 0.2 dB and 0.8 ° respectively.

A comparison table (Table-1 is added to put our work in the context of relevant published papers in this frequency range. The design presented in this paper covers fractional bandwidth of approximately 37% around the center frequency, 220-320 GHz, which is promising at this frequency range. Moreover, the proposed fabrication method demonstrates a fast and simple fabrication method with high fabrication accuracy. Work presented at [26] has good performance above 200 GHz but the fabrication method is a time intense process. On the other hand, the divider in [25] has shown better reflection coefficient but it operates below 200 GHz. Also, they have used substrate-based elements in a waveguide structure to provide the output port's isolation and matching. Furthermore, this new fabrication method opens a new door to fabricate passive components at mmWave and sub-mmWave frequencies in a straightforward way.

V. CONCLUSION

A RGW power divider fabricated by dry film photoresist-based micromachining has been presented. For the proposed power divider, the waveguide port is located at the top plate which simplifies the transition between the RW to the GW structure. The measured transmission coefficients are equal to -3.5 ± 0.4 dB at 220-325 GHz and the measured input reflection coefficient is below −12 dB at 220-325 GHz. The proposed fabrication process can deliver structures with high accuracy. Also, the fabrication method is simple and not very time intense.

ACKNOWLEDGMENT

The authors would like to thank the nanofabrication laboratory personnel at the Chalmers University of Technology for their help with the fabrication process.

REFERENCES

[1] D. Lockie and D. Peck, "High-data-rate millimeter-wave radios," *IEEE Microw. Mag.*, vol. 10, no. 5, pp. 75–83, Aug. 2009.

[2] M. Alonso-del Pino, C. Jung-Kubiak, T. Reck, C. Lee, and G. Chattopadhyay, "Micromachining for advanced terahertz: Interconnects and packaging techniques at terahertz frequencies," *IEEE Microw. Mag.*, vol. 21, no. 1, pp. 18–34, Jan. 2020.

[3] P. Liu, "Millimeter-wave planar antenna array based on modified bulk silicon micromachining technology," *IEEE Trans. Antennas Propag.*, vol. 68, no. 11, pp. 7676–7681, 2020.

[4] Y. Li and P. L. J. Kirby Papapolymerou, "Silicon micromachined W-band folded and straight waveguides using DRIE technique," in *IEEE MTT-S Int. Microw. Symp. Dig.*, Jun. 2006, pp. 1915–1918.

[5] T. Yingtao, "Investigation of SU8 as a structural material for fabricating passive millimeter-wave and terahertz components," *J. Micro/Nanolithography, MEMS*, vol. 14, no. 4, pp. 1–9, 2015.

[6] C. H. Smith and N. S. Barker, "SU-8 micromachining process for millimeter and submillimeter-wave waveguide circuit fabrication," in *Proc. 33rd Int. Conf. Infr., Millim. THz Waves*, Sep. 2008.

[7] W. Ehrfeld, "Materials of LIGA technology," *Microsyst. Technol.*, vol. 5, no. 3, pp. 105–112, 1999.

[8] Y.-S. Liao and Y.-T. Chen, "Precision fabrication of an arrayed micro metal probe by the laser-LIGA process," *J. Micromech. Microeng.*, vol. 15, no. 12, pp. 2433–2440, Dec. 2005.

[9] P. L. Kirby, D. Pukala, H. Manohara, I. Mehdi, and J. Papapolymerou, "Characterization of micromachined silicon rectangular waveguide at 400 GHz," *IEEE Microw. Wireless Compon. Lett.*, vol. 16, no. 6, pp. 366–368, Jun. 2006.

[10] G. Chattopadhyay, J. S. Ward, H. Manohara, and R. Toda, "Deep reactive ion etching based silicon micromachined components at terahertz frequencies for space applications," in *Proc. 33rd Int. Conf. Infr., Millim. THz Waves*, Sep. 2008, pp. 1–2.

[11] C. D. Nordquist, M. C. Wanke, A. M. Rowen, C. L. Arrington, M. Lee, and A. D. Grine, "Design, fabrication, and characterization of metal micromachined rectangular waveguides at 3 THz," in *Proc. IEEE Antennas Propag. Soc. Int. Symp.*, Jul. 2008, pp. 1–4.

[12] S. Abada, L. Salvi, R. Courson, E. Daran, B. Reig, J. B. Doucet, T. Camps, and V. Bardinal, "Comparative study of soft thermal printing and lamination of dry thick photoresist films for the uniform fabrication of polymer MOEMS on small-sized samples," *J. Micromech. Microeng.*, vol. 27, no. 5, May 2017, Art. no. 055018.

[13] S. Farjana, S. Rahiminejad, A. U. Zaman, J. Hansson, M. A. Ghaderi, S. Haasl, and P. Enoksson, "Polymer based 140 GHz planar gap waveguide array antenna for line of sight (LOS) MIMO backhaul links," in *IEEE MTT-S Int. Microw. Symp. Dig.*, Jul. 2019, pp. 148–150.

[14] S. Farjana, M. Ghaderi, S. Rahiminejad, S. Haasl, and P. Enoksson, "Dry film photoresist-based microfabrication: A new method to fabricate millimeter-wave waveguide components," *Micromachines*, vol. 12, no. 3, p. 260, Mar. 2021.

[15] E. Rajo-Iglesias, M. Ferrando-Rocher, and A. U. Zaman, "Gap waveguide technology for millimeter-wave antenna systems," *IEEE Commun. Mag.*, vol. 56, no. 7, pp. 14–20, Jul. 2018.

[16] A. Vosoogh, "Compact integrated full-duplex gap waveguide-based radio front end for multi-gbit/s point-to-point backhaul links at E-band," *IEEE Trans. Microw. Theory Techn.*, vol. 67, pp. 3783–3797, Jun. 2019.

[17] M. Ferrando-Rocher, "8×8 Ka-band dual-polarized array antenna based on gap waveguide technology," *IEEE Trans. Antennas Propag.*, vol. 67, no. 7, pp. 4579–4588, Oct. 2019.

[18] R. Maaskant, "Spatial power combining and splitting in gap waveguide technology," *IEEE Microw. Wireless Compon. Lett.*, vol. 26, no. 7, pp. 472–474, Oct. 2016.

[19] S. Rahiminejad, E. Pucci, S. Haasl, and P. Enoksson, "SU8 ridge-gap waveguide resonator," *Int. J. Microw. Wireless Technol.*, vol. 6, no. 5, pp. 459–465, 2014.

[20] S. Farjana, M. Ghaderi, A. U. Zaman, S. Rahiminejad, T. Eriksson, J. Hansson, Y. Li, T. Emanuelsson, S. Haasl, P. Lundgren, and P. Enoksson, "Realizing a 140 GHz gap Waveguide–Based array antenna by low-cost injection molding and micromachining," *J. Infr., Millim., THz Waves*, vol. 42, no. 8, pp. 893–914, Aug. 2021.

[21] S. Rahiminejad, A. U. Zaman, E. Pucci, H. Raza, V. Vassilev, S. Haasl, P. Lundgren, P.-S. Kildal, and P. Enoksson, "Micromachined ridge gap waveguide and resonator for millimeter-wave applications," *Sens. Actuators A, Phys.*, vol. 186, pp. 264–269, Oct. 2012.

[22] S. H. Shehab and N. C. J. Karmakar Walker, "Substrate-integrated-waveguide power dividers: An overview of the current technology," *IEEE Antennas Propag. Mag.*, vol. 62, no. 4, pp. 27–38, Oct. 2020.

[23] S. Farjana, "Low loss gap waveguide transmission line and transitions at 220–320 GHz using dry film micromachining," *IEEE Trans. Compon., Packag., Manuf. Technol.*, vol. 11, no. 11, pp. 2012–2021, Nov. 2021.

[24] V. Vassilev, V. Belitsky, D. Urbain, and S. Kovtonyuk, "A new 3-dB power divider for millimeter-wavelengths," *IEEE Microw. Wireless Compon. Lett.*, vol. 11, no. 1, pp. 30–32, Jan. 2001.
[25] A. Gouda, C. Lopez, V. Desmaris, D. Meledin, A. Pavolotsky, and V. Belitsky, "Millimeter-wave wideband waveguide power divider with improved isolation between output ports," *IEEE Trans. Thz Sci. Technol.*, vol. 11, no. 4, pp. 408–416, Jul. 2021.
[26] R. Malmqvist, A. Gustafsson, J. Svedin, B. Beuerle, U. Shah, and J. Oberhammer, "A 220–325 GHz low-loss micromachined waveguide power divider," in *Proc. IEEE Asia Pacific Microw. Conf. (APMC)*, Nov. 2017, pp. 291–294.

SADIA FARJANA was born in Bangladesh. She received the B.Sc. degree in electrical and electronics engineering from the Chittagong University of Engineering and Technology, and the M.Sc. degree in microtechnology from the Chalmers University of Technology, Gothenburg, Sweden, where she is currently pursuing the Ph.D. degree. Her research interests include the field of micro and nano-system technology and fabrication.

ASHRAF UZ ZAMAN (Senior Member, IEEE) was born in Chittagong, Bangladesh. He received the B.Sc. degree in electrical and electronics engineering from the Chittagong University of Engineering and Technology, Chittagong, and the M.Sc. and Ph.D. degrees from the Chalmers University of Technology, Gothenburg, Sweden, in 2007 and 2013, respectively. He is currently an Associate Professor with the Communication and Antenna Systems Division, Chalmers University of Technology. His current research interests include millimeter-wave planar antennas in general, gap waveguide technology, frequency-selective surfaces, microwave passive components, and packaging techniques and integration of MMICs with the antennas.

PER LUNDGREN received the Ph.D. degree from the Chalmers University of Technology, Sweden, in 1996. His technical expertise is in the field of solid state electronics, where he focuses on integration challenges for novel nanostructures in electronics. Since 2000, he has been holding a position as an Associate Professor with the Chalmers University of Technology.

PETER ENOKSSON (Member, IEEE) received the Master of Science degree in engineering physics, in 1986, and the Ph.D. degree from the KTH Royal Institute of Technology, Stockholm, Sweden, in 1997.

In 1997, he was appointed as an Assistant Professor, and then became an Associate Professor with KTH, in 2000. In 2001, he was appointed as a Professor in MEMS/MOEMS with the Chalmers University of Technology, Gothenburg, Sweden. In 2002 and 2004, he was the Vice Dean of the School of Electrical Engineering and the Head of the Solid State Electronics Laboratory, from 2003 to 2006. He was the Head of the Microsystem and Nanosystems Group, Department of Microtechnology and Nanoscience, MC2. He is an Initiator of spin-off companies. He has authored over 300 research journals and conference papers and holds more than ten patents. His current research interests include energy storage, metamaterials, and MEMS/NEMS with other sciences in novel dedicated and advanced systems. He was a recipient of the Innovation Cup. He is a referee of several journals and also a member of the Editorial Board of the *Journal of Micromechanics and Microengineering*.